Onik et al., J Clin Exp Pathol 2017, 7:4
DOI: 10.4172/2161-0681.1000319

Journal of Clinical & Experimental Pathology

Research Article Open Access

# Electrical Membrane Breakdown (EMB): Preliminary Findings of a New Method of Non-thermal Tissue Ablation

**Onik GM[1,2], Bostwick DG[1]*, Miessau JA[1] , Webb Z[3] and Friedman MB[4]**

[1]RFEMB Holdings, LLC, 4724 Lake Calabay Drive, Orlando, FL, USA
[2]Department of Mechanical Engineering, Carnegie Mellon University, Pittsburgh PA, USA
[3]Department of Pathology, University of Oklahoma School of Medicine, Oklahoma City, OK, USA
[4]Department of Diagnostic Radiology, Veterans Administration Connecticut Health Care System, Yale University School of Medicine, West Haven, CT, USA

## Abstract

Electrical membrane breakdown (EMB) is a novel form of non-thermal treatment that has not, to our knowledge, been previously evaluated for its potential utility as an ablation mechanism. The findings with EMB immediately after treatment were compared with other forms of ablation (cryoablation and IRE (irreversible electroporation)) in the porcine liver clinically, ultrasonographically, and by light microscopy and ultrastructural analysis. Clinically, EMB did not induce muscular contractions, in contrast with IRE. By ultrasound, all lesions were hypoechoic when compared to the untreated liver. EMB created a consistent pattern of immediate tissue destruction at the light microscopic and ultrastructural level, characterized by pulse-dose-related coagulative necrosis and nuclear pyknosis, preserved blood vessels and adjacent structures, and sharply demarcated margins. We conclude that the profile of EMB ablation is distinctive and unique, inducing necrosis by immediate electrical rupture of cell membranes non-thermally while preserving proteins and adjacent vessels with potentially superior stimulation of the immune system than other ablation modalities.

**Keywords:** Pathology; Electrical; Ultrastructure; Animal; Radiofrequency; Electroporation

**Abbreviations:** DC: Direct Current; HIFU: High-Intensity Focused Ultrasound; IRE: Irreversible Electroporation; kHZ: Kilohertz; N-TIRE: Non-thermal Irreversible Electroporation; RF: Radiofrequency; EMB: Electrical Membrane Breakdown; µm: Microns; µs: Microseconds; V: Volts.

## Introduction

Ablation is a surgical technique for destroying unwanted cells or organs, including abnormal growths such as cancer. Unlike surgical extirpation, ablation does not remove the treated tissue; instead, the altered cell mass persists in situ, with subsequent removal or sequestration by the body's defense and healing mechanisms. This creates an opportunity to harness the immune system to recognize the dead cells and auto-immunize the body against potential cancer neo-antigens [1].

We sought to identify a novel method of ablation with a unique treatment profile unlike any other form of ablation that may be useful in combination with cancer immunotherapy: electrical tissue destruction that induces necrosis, stimulates the immune system, preserves proteins and cancer neo-antigens owing to non-thermal injury, and spares adjacent structures such as blood vessels from alteration. By preserving the protein structure and antigenicity of cancer cell membranes and intracellular contents, this novel method of non-thermal ablation should theoretically provoke the abscopal effect in distant cancer deposits (metastases) containing similar neo-antigens, thereby exploiting the immune system in killing cancer. The only other electrical ablation technique that is non-thermal (irreversible electroporation, or IRE) results in only a modest immune response owing to mechanism of cell death by apoptosis, so it would be less suitable for use in combination with immune treatment of cancer metastases [2].

In this report, we describe the immediate histopathologic and ultrastructural effects of EMB in an animal model (porcine liver) that closely mimics human tissue [3]. The findings were compared and contrasted with cryoablation, IRE, and other forms of ablation at the light microscopic and ultrastructural level to document the mechanism of cell damage. We found that EMB induced a novel pattern of cellular injury with immediate necrosis and non-thermal cell death while preserving blood vessels and nerves.

### Aims of the study

- Identify the light microscopic and ultrastructural findings with electrical membrane breakdown (EMB).
- Compare the morphologic findings of EMB with cryoablation and irreversible electroporation.

## Materials and Methods

### Animals

Three female Yorkshire/Landrace hybrid pigs (40-60 kg) were obtained from an approved local vendor and placed in quarantine prior to experimentation. Study was conducted under the auspices of the Animal Care and Use Committee of the Celebration Florida Nicholson Center (Celebration, FL) in accordance with Good Laboratory Practice regulations as set forth by the 21 Code of Federal Regulations (CFR) Part 58 (Protocol Number 2016.08.01). Animals were placed under general anesthesia using desflourane. In addition, pancuronium (0.1 mg/kg, at a dose of 1 mg/ml) was administered through an IV prior to the procedure to reduce muscle contractions during the application of the DC electrical pulses used for creating the IRE lesions. Pancuronium

***Corresponding author:** David G. Bostwick, RFEMB Holdings, 4724 Lake Calabay Drive, Orlando, FL 32837, USA, Tel: 804-677-8527; E-mail: dbostwick@grangergenetics.com

**Received** July 07, 2017; **Accepted** August 02, 2017; **Published** August 07, 2017

**Citation:** Onik GM, Bostwick DG, Miessau Esq JA, Webb Z, Friedman MB (2017) Electrical Membrane Breakdown (EMB): Preliminary Findings of a New Method of Non-thermal Tissue Ablation. J Clin Exp Pathol 7: 319. doi:10.4172/2161-0681.1000319

**Copyright:** © 2017 Onik GM, et al. This is an open-access article distributed under the terms of the Creative Commons Attribution License, which permits unrestricted use, distribution, and reproduction in any medium, provided the original author and source are credited.

(0.05 mg/ml at 1 mg/ml) was administered throughout the procedure as needed. The liver was exposed via a midline incision. The entire procedure took less than three hours per pig. Upon completion of the ablation, animals were immediately sacrificed prior to their recovery from anesthesia.

### Ablation methods

Three ablation methods (EMB [electrical membrane breakdown], cryoablation, and IRE [irreversible electroporation]) were employed.

EMB (electric membrane breakdown) consists of application of short, high-voltage radiofrequency pulses with instant charge reversal and a square wave form, producing high electric fields between two electrodes. Process parameters such as electric field strength, pulse width, pulse number, wave shape, and frequency were important in optimizing desired output. For our application of EMB, we used a patented device (RFEMB Holdings, LLC, Orlando, FL) [4]. Temperatures were continuously monitored using an optical temperature monitoring system from Omega Engineering, Norwalk CT. Temperatures were monitored for the center of the lesion and at each electrode. Temperature was maintained below 42 degrees centigrade at all times.

Cryoablation was performed according to the manufacturer's recommendations (Endocare, Inc., Irvine, CA).

IRE (irreversible electroporation) was performed using 18 gauge stainless steel electrodes (Angiodynamics Inc, Latham, NY) with sliding insulating sheaths exposing 1 cm of each electrode, as previously described [5]. The electrodes were inserted in the liver under ultrasound monitoring with two electrodes in a roughly axial parallel configuration. Square DC pulses were applied to the liver through the electrodes using a DC pulse generator. Electrical pulses were delivered in a bipolar manner between two electrodes.

### Ultrasound

Ultrasound imaging was performed with Noblus Hitachi Ultrasound machine (Hitachi Healthcare Americas, Twinsburg, OH) using a multifrequency endfire intracavitary transducer. Ultrasonographic studies were obtained directly from the liver immediately after each ablation and before each animal was sacrificed to determine if the effects of EMB can be monitored by medical imaging.

### Pathology and ultra-structural studies

Upon completion of each ablation method, superficial 2.0 X 2.0 X 1.0 cm slices of liver tissue were obtained for pathologic analysis to encompass the maximum area of gross abnormality; elapsed time from treatment to biopsy was less than 30 min. In all instances, tissue was trimmed and then immediately immersed in 10% neutral phosphate buffered formalin for light microscopic analysis; in six instances, tissue was also minced into 1 mm blocks and immersed immediately in a mixture of 4% formaldehyde and 1% glutaraldehyde for ultrastructural analysis. A slice of non-ablated liver was separately submitted as a presumptive normal control.

For light microscopy, tissue specimens were routinely processed through graded alcohols and xylene, embedded in paraffin, sliced at 3 microns, and stained with hematoxylin and eosin.

For ultrastructural studies, specimens were routinely processed, stained with uranyl acetate, and examined in a JEOL (Tokyo, Japan) transmission electron microscopy at magnifications ranging from 5000X to 60,000X.

## Results

### Clinical findings

For IRE, we were unable to make the neuromuscular blockade complete with standard dosages of medication during the application of the DC pulses. Conversely, EMB showed no evidence of muscular contractions at the same voltages even in the absence of neuromuscular blockade.

### Ultrasound findings

All lesions were hypoechoic when compared to the untreated liver, irrespective of the modality employed.

### Light microscopic findings

Normal porcine liver: The normal porcine liver was remarkably similar in histologic architecture and cellular detail to the human liver, as previously described [3], consisting of lobules of confluent hexagonal plates of hepatocytes with innermost central veins. At the vertices of the lobules, the portal triads included the bile ducts, hepatic arteries and hepatic portal veins. Inflammation was absent (Table 1).

EMB (100 pulses) 90 µs pulse width, 250 kHZ, 2000 V: There were

| | Tissue and cell necrosis | Disorganization of lobular plates | Hepatocyte shrinkage | Destruction of vessels and nerves | Vascular Congestion | Venous thrombosis | Inflammation | Nuclear Findings | Mitochondrial Changes | Cell membrane changes | Cytoplasmic Vacuoles Present |
|---|---|---|---|---|---|---|---|---|---|---|---|
| Untreated porcine liver | N | N | N | N | N | N | N | N | N | N | N |
| EMB (100 pulses) | N | N | N | N | Y | N | N | N | Mild Changes | N | N |
| EMB (1500 pulses) | Y | Y | Y | N | Y | N | N | Shrinkage and early pyknosis | Y | N | N |
| EMB (4000 pulses) | Y | Y | Y | N | Y | Y | N | Pyknosis | Complete destruction | Complete destruction | N |
| Cryoablation | Y | Y | Y | Y | Y | Y | N | N | Complete destruction | Complete destruction | Rare, large |
| IRE (99 pulses)[a] | N | N | N | N | Y | N | N | N | Minimal changes | N[b] | N |

[a]Submitted for light microscopy only; ultrastructural findings derived from the literature.
[b]The cell and nuclear membranes appeared intact by routine light microscopy and transmission electron microscopy; it should be noted that electroporation is best visualized by scanning electron microscope, so such findings would not be evident in our studies.

**Table 1:** Light microscopic and ultrastructural findings with EMB, cryoablation, and IRE.

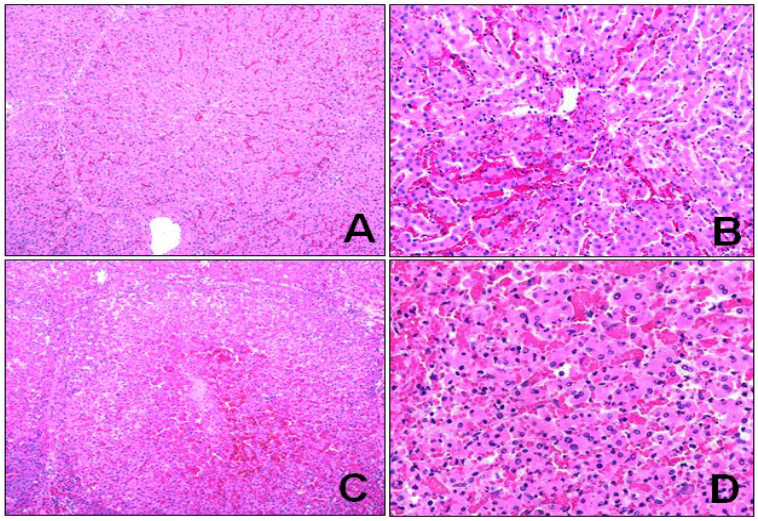


**Figure 1:** EMB-induced changes in the porcine liver, light microscopy. A: 100 pulses: Intact hepatic lobule with moderate vascular congestion. (Hematoxylin & eosin, magnification 100X) B: 100 pulses: Centrilobular region, with intact central vein (just above center of image) and vascular congestion. Hepatocytes are morphologically unaltered (hematoxylin & eosin, magnification 200X). C: 4000 pulses: There is pan-lobular coagulative necrosis and vascular congestion with a thin-rim of intact hepatic parenchyma at the periphery (hematoxylin & eosin, magnification 100X). D; 4000 pulses: Vascular congestion, with hepatocytes in disarray and shrunken, displaying pyknotic nuclei (hematoxylin & eosin, magnification 400X).

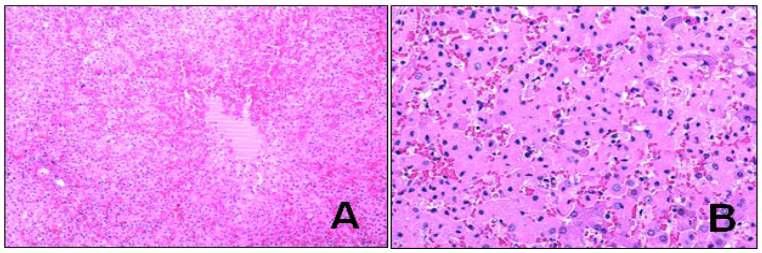


**Figure 2:** Cryoablation-induced changes, light microscopy. A. There is marked congestion and coagulative necrosis of the entire lobule (hematoxylin & eosin, magnification 100X). B: Vascular congestion with fused disorganized hepatocytes displaying shrunken pyknotic nuclei (hematoxylin & eosin, magnification 400X).

minimal architectural and cytologic changes, the most prominent of which was vascular congestion (Figure 1A-D). No inflammation was observed.

EMB (1500 pulses) 90 μs pulse width, 250 kHZ, 2000 V: The lobular architecture was disorganized and chaotic, with marked vascular congestion, although vascular structures appeared intact. There was no inflammation. Hepatocyte nuclei were shrunken and hyperchromatic, cellular organelles such as mitochrondria were distorted, and cell membranes were indistinct. At the margins, there was a sharp demarcation between altered and un-altered tissue (less than 50 microns).

EMB (4000 pulses) 90 μs pulse width, 250 kHZ, 2000 V: There was massive cell death (coagulative necrosis) with loss of the lobular architecture accompanied by marked vascular congestion. Vessels and bile ducts in the portal triads were preserved, as were the central veins, although venous thrombosis was focally present. No inflammation was observed. Hepatocyte nuclei were pyknotic, mitochondria and cellular organelles were destroyed, and cell membranes were obliterated. No cytoplasmic vacuoles, monophasic glycogen granules, or electron-dense lysosomes were observed. At the margins, there was a sharp demarcation between altered and un-altered tissue (Figure 1).

Cryoablation: The liver showed mummification (coagulative necrosis), with complete cell death, marked vascular congestion and occasional scattered intermediate size and large vacuoles within hepatocytes; There was no thrombosis, but vessels were mummified, including pyknotic nuclei as well as loss of staining of nuclei, creating pale "ghost"nuclei. At the margins, there was a thin line of demarcation between altered and un-altered tissue (Figure 2A and B).

IRE (99 pulses) DC pulses, 90 μs pulse width 2000V: There were minimal changes, including vascular congestion and minimal distortion of scattered mitochondrial cristae. No vacuolization was observed. All adjacent structures, including blood vessels, were intact (Figure 3).

## Ultra structural findings

EMB (100 pulses): Architecture and cell and nuclear membranes were preserved, with vascular congestion and the appearance of occasional scattered microvesicles at the periphery of intact cells (Figure 4A). Mitochondria were mildly distorted.

EMB (1500 pulses): Architecture was distorted, accompanied by prominent vascular congestion. The most striking finding was alteration of mitochondria, with marked enlargement and destruction of cristae in about half of cells. Cytoplasmic blebs were occasionally observed at the edge of some hepatocytes.

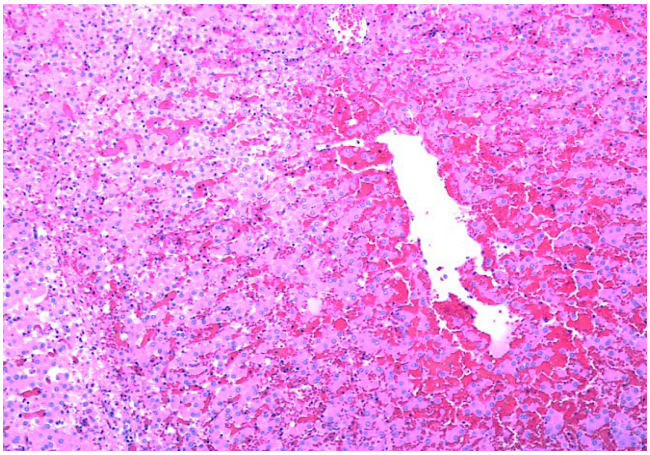

**Figure 3:** IRE-induced changes, light microscopy. Intact lobular architecture with prominent vascular congestion (hematoxylin & eosin, magnification 200X).

EMB (4000 pulses): There was marked distortion of all cells and internal organelles, including disorganization, complete loss of cell junctions, mummification of cytoplasmic contents with loss of resolution and early vacuolization of mitochondria, and loss of microvilli around bile ductules (Figure 4B). Cell membranes were fuzzy and indistinct.

Cryoablation: There was coagulative necrosis, characterized by architectural distortion and loss of cell integrity, including mummification of cytoplasmic contents and marked alteration of mitochondrial contours and cristae (Figure 5). There was also prominent vascular congestion.

## Discussion

Our results showed that EMB created a consistent pattern of immediate tissue destruction at the light microscopic and ultrastructural level, characterized by pulse dose-related coagulative necrosis and nuclear pyknosis. Unlike cryoablation and most other forms of tissue ablation, EMB preserved blood vessels, bile ducts, and nerves,

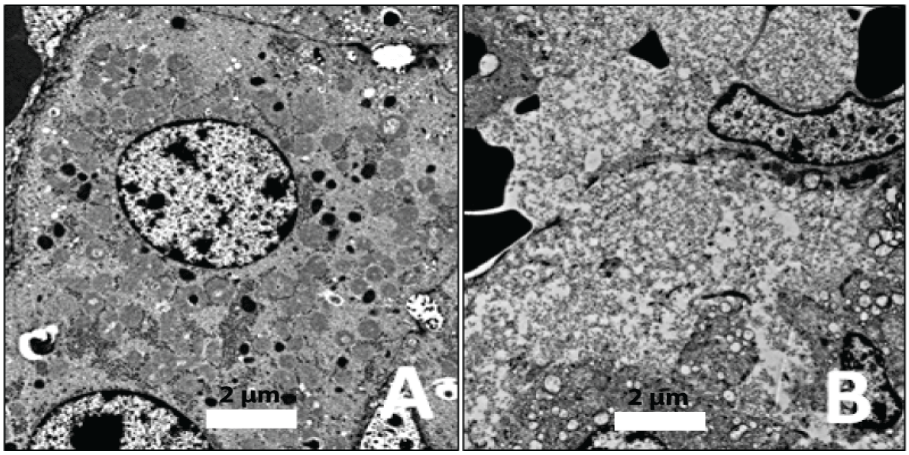


**Figure 4:** EMB-induced changes, electron microscopy. A: 100 pulses: Intact cell and nuclear membranes preserved, with scattered microvesicles at the periphery of intact cells. Mitochondria are mildly distorted. Note intact microvilli of bile canaliculus in lower right (magnification, 8000X). Bar 2 µm. B: 4000 pulses: Coagulative necrosis, with loss of architectures and destruction of organelles and cell membranes. Vacuoles present within many of the cells (magnification, 8000X). Bar 2 µm.

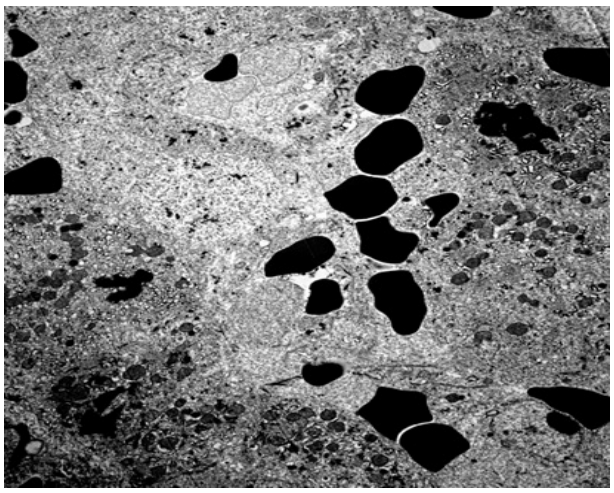

**Figure 5:** Cryoablation-induced changes, electron microscopy. Coagulation necrosis accompanied by vascular congestion (magnification, 4000X). Bar, 2 µm.

indicating preferential destruction of hepatocytes. To our knowledge, these findings are the first to demonstrate the potential utility of EMB as a new form of non-thermal tissue ablation that may have clinical value.

We confirmed that IRE, the only other electrical non-thermal form of tissue ablation, did not induce necrosis or pyknotic (morphologically dead or dying) nuclei immediately after treatment, similar to previous descriptions [6,7]. These findings reflected differences in mechanism of cell death between EMB and IRE (immediate necrosis vs. apoptosis, respectively) (Table 2). However, both treatments preserved surrounding tissues, thereby avoiding the heat sink effect [8] and both were sharply demarcated, with no apparent transition zone with alteration at the margins.

EMB did not induce muscular contractions, even in the absence of neuromuscular blockade, in contrast with IRE. This is an important distinction, as IRE requires the administration of general anesthesia and paralytic agents in order to eliminate muscle contractions [9].

There are numerous methods of ablation that vary by mechanism of tissue destruction (chemical, thermal, electrical), rapidity of cell death (apoptosis: slow [1-3 days]; necrosis: immediate), effect on native proteins (intact or denatured); differential sparing of adjacent structures such as blood vessels and nerves (intact or ablated); and likely impact on the immune system (non-stimulatory or stimulatory) (Table 3). The four requirements for activation of the acquired immune system are antigen presentation, antigen recognition by T-cells, interaction of costimulatory molecules, and the presence of danger signals [10] and the method of ablation likely influences these factors. For example, protein denaturation by ablation may interfere with antigen presentation or recognition. Thermal ablation methods such as hyperthermia and cryoablation under clinically used protocols irreversibly alter the three dimensional protein structures and destroy the structure of antigenic determinants [11], whereas non-thermal methods of ablation such as IRE and EMB theoretically preserve native proteins and cancer neo-antigens. Ablation may also result in rapid cell death (necrosis) or slow programmed cell death (apoptosis), but only necrosis is thought to stimulate a substantial immune response. Mehta et al. noted that apoptotic cell death eliminated danger signals (e.g., production of heat shock proteins) and blocked antigen presentation because phagocytosis shielded intracellular contents; [12] also; dendritic cells that take ingest apoptotic cells do not mature, may have suppressed cytokine production, and may trigger clonal deletion and anergy. Conversely, necrosis caused cell rupture with subsequent spilling of intracellular contents into the extracellular environment and likely migration and activation of dendritic cells with subsequent stimulation of cytotoxic T cells.

Our study has multiple limitations. In this preliminary report, we restricted study to a single species and single tissue type, and employed only a modest number of animals and specimens. Despite the well-recognized histologic similarity between the porcine and human liver, our findings in the pig may not apply in humans. We limited our study to the changes immediately following treatment, but it would be useful to have multiple time points after treatment to determine the full extent of damage and thereby confirm the mechanisms of cell death. We employed only a single skilled operator (Dr. Onik), and these results may differ according to the expertise of the surgeon. Finally, only a limited number of EMB variables were studied (e.g., duration of treatment, wave shapes created, combinations of treatments, etc.) so these results should be considered preliminary, albeit novel. It should also be noted that we have not directly studied the effect of our treatments on cancer neo-antigens and protein structure, so any hypotheses regarding potential utility of ablation in harnessing the immune response should be considered speculative [13-20].

| Gross Findings | LIGHT and ELECTRON Microscopic Findings |
|---|---|
| **IRE** | |
| Acute[a] | None other than vascular congestion: distinctive diffuse membrane pores ultrastructurally (11) |
| Delayed[b] | Apoptopic cell death: Hepatocytenecrosis: Blood vessels and nerves preserved: resolution of inflammation within a few weeks (3,5,6,11,12); conversion to fibrosis. |
| **EMB** | |
| Acute[a] | Coagulation necrosis with nuclear pyknosis; blood vessels and nerves preserved |
| Delayed[b] | Unknown; assume resorption of necrotic tissue or conversion to fibrosis. |
| IRE: Irreversible electroporation; N-TIRE: Non-thermal IRE; EMB: Electrical membrane breakdown.<br>[a]Acute refers to immediate post-operative period (up to 1 hour after treatment); [b]Delayed refers to late changes (hours to days or more after treatment), allowing for effects of regeneration. | |

**Table 2:** Comparison of electrical non-thermal tissue ablation methods.

| Method | Mechanism | Description |
|---|---|---|
| **Thermal** | | |
| Microwave [13] | Heat and Mechanical | Creates coagulation necrosis with friction and heat |
| HIFU [14] | Heat | Creates necrosis by focusing energy into a small area creating heat |
| Laser [15] | Heat | Creates necrosis with light energy |
| RF Thermal [15] | Heat and mechanical | Creates cellular desiccation and protein coagulation |
| Steam [16] | Heat | Creates coagulation necrosis with heat |
| Cryosurgery [15] | Cold | Creates necrosis by dehydration and ice formation |
| **Non-Thermal** | | |
| Alcohol, Hypertonic Saline, Acetic Acid Injections [17] | Chemical | Creates coagulative necrosis *via* dehydration and protein coagulation |
| Photodynamic [18] | Chemical | Creates cell damage by producing reactive oxygen species and destroying vasculature |
| IRE and N-TIRE [3-6,11,12] | Electrical | Creates apoptosis with preservation of vessels; delayed necrosis |
| EMB | Electrical | Creates necrosis with preservation of vessels |
| HIFU: High-intensity focused ultrasound; IRE: Irreversible electroporation; N-TIRE: Non-Thermal irreversible electroporation; EMB: Electrical Membrane Breakdown. | | |

**Table 3:** Comparison of common tissue ablation methods.

## Conclusion

EMB is a novel form of non-thermal tissue ablation that results in immediate coagulative necrosis while preserving adjacent structures. It is distinguished from IRE by a unique mechanism of non-thermal cell destruction and characteristic electrical properties that avoid muscular contractions during treatment.

### Declaration of Conflicting Interests

DGB, GO, and JM are affiliated and have a personal financial interest, including patents, in RFEMB Holdings, LLC, a company that was established to commercialize the technology of electrical membrane breakdown (EMB). Each of these authors has signed the following: "I had full access to all of the data in this study and I take complete responsibility for the integrity of the data and the accuracy of the data analysis."

ZW and MBF declare that they have no conflicting interests.

### Funding Source

Funding was provided by RFEMB Holdings, LLC, Orlando, FL.

### References

1. Veenstra JJ, Gibson HM, Freytag S, Littrup PJ, Wei WZ (2015) In situ immunization via non-surgical ablation to prevent local and distant tumor recurrence. Oncoimmunology 4: e989762.
2. Al-Sakere B, Bernat C, Andre F, Connault E, Opolon P, et al. (2007) A study of the immunological response to tumor ablation with irreversible electroporation. Technol Cancer Res Treat 6: 301-306.
3. Flaks B (1971) Observations on the fine structure of the normal porcine liver. J Anat 108: 563-577.
4. Onik GM, Miessau JA (2015) System and Method For Creating Radio-Frequency Energy Electrical Membrane Breakdown For Tissue Ablation. U.S. Patent and Trademark Office.
5. Rubinsky B, Onik G, Mikus P (2007) Irreversible electroporation: a new ablation modality--clinical implications. Technol Cancer Res Treat 6: 37-48.
6. Li X, Xu K, Li W, Qiu X, Ma B, et al. (2012) Immunologic response to tumor ablation with irreversible electroporation. PLoS One 7: e48749.
7. Vogel JA, van Veldhuisen E, Agnass P, Crezee J, Dijk F, et al. (2016) Time-Dependent Impact of Irreversible Electroporation on Pancreas, Liver, Blood Vessels and Nerves: A Systematic Review of Experimental Studies. PLoS One 11: e0166987.
8. Lee EW, Loh CT, Kee ST (2007) Imaging guided percutaneous irreversible electroporation: ultrasound and immunohistological correlation. Technol Cancer Res Treat 6: 287-294.
9. Arena CB, Sano MB, Rossmeisl JH, Caldwell JL, Garcia PA, et al. (2011) High-frequency irreversible electroporation (H-FIRE) for non-thermal ablation without muscle contraction. Biomed Eng Online 10: 102.
10. Bastianpillai C, Petrides N, Shah T, Guillaumier S, Ahmed HU, et al. (2015) Harnessing the immunomodulatory effect of thermal and non-thermal ablative therapies for cancer treatment. Tumour Biol 36: 9137-9146.
11. Clasen S, Krober SM, Kosan B, Aebert H, Fend F, et al. (2008) Pathomorphologic evaluation of pulmonary radiofrequency ablation: proof of cell death is characterized by DNA fragmentation and apoptotic bodies. Cancer 113: 3121-3129.
12. Mehta A, Oklu R, Sheth RA (2016) Thermal Ablative Therapies and Immune Checkpoint Modulation: Can Locoregional Approaches Effect a Systemic Response? Gastroenterol Res Pract 2016: 9251375.
13. Thomson KR, Kavnoudias H, Neal RE (2015) Introduction to Irreversible Electroporation--Principles and Techniques. Tech Vasc Interv Radiol 18: 128-134.
14. Onik G, Mikus P, Rubinsky B (2007) Irreversible electroporation: implications for prostate ablation. Technol Cancer Res Treat 6: 295-300.
15. Bostwick DG, Larson TR (1995) Transurethral microwave thermal therapy: pathologic findings in the canine prostate. Prostate 26: 116-122.
16. Van Leenders GJ, Beerlage HP, Ruijter ET, de la Rosette JJ, van de Kaa CA (2000) Histopathological changes associated with high intensity focused ultrasound (HIFU) treatment for localised adenocarcinoma of the prostate. J Clin Pathol 53: 391-394.
17. Gravante G, Sconocchia G, Ong SL, Dennison AR, Lloyd DM (2009) Immunoregulatory effects of liver ablation therapies for the treatment of primary and metastatic liver malignancies. Liver Int 29: 18-24.
18. Roy S (2013) Focal hydrothermal ablation: preliminary investigation of a new concept. Cardiovasc Intervent Radiol 36: 1112-1119.
19. Rehman J, Landman J, Lee D, Venkatesh R, Bostwick DG, et al. (2004) Needle-based ablation of renal parenchyma using microwave, cryoablation, impedance- and temperature-based monopolar and bipolar radiofrequency, and liquid and gel chemoablation: laboratory studies and review of the literature. J Endourol 18: 83-104.
20. Kleinovink JW, van Driel PB, Snoeks TJ, Prokopi N, Fransen MF, et al. (2016) Combination of Photodynamic Therapy and Specific Immunotherapy Efficiently Eradicates Established Tumors. Clin Cancer Res 22: 1459-1468.